

Advanced cathode materials for high-power applications

K. Amine*, J. Liu, I. Belharouak, S.-H. Kang, I. Bloom, D. Vissers, G. Henriksen

Argonne National Laboratory, 9700 S. Cass Ave., Argonne, IL 60439, USA

Available online 8 August 2005

Abstract

In our efforts to develop low cost high-power Li-ion batteries with excellent safety, as well as long cycle and calendar life, lithium manganese oxide spinel and layered lithium nickel cobalt manganese oxide cathode materials were investigated. Our studies with the graphite/LiPF₆/spinel cells indicated a very significant degradation of capacity with cycling at 55 °C. This degradation was caused by the reduction of manganese ions on the graphite surface which resulted in a significant increase of the charge-transfer impedance at the anode/electrolyte interface. To improve the stability of the spinel, we investigated an alternative salt that would not generate HF acid that may attack the spinel. The alternative salt we selected for this work was lithium bisoxalato borate, LiB(C₂O₄)₂ (“LiBoB”). In this case, the graphite/LiBoB/spinel Li-ion cells exhibited much improved cycle/calendar life at 55 °C and better abuse tolerance, as well as excellent power. A second system based on LiNi_{1/3}Co_{1/3}Mn_{1/3}O₂ layered material was also investigated and its performance was compared to commercial LiNi_{0.8}Co_{0.15}Al_{0.05}O₂. Cells based on LiNi_{1/3}Co_{1/3}Mn_{1/3}O₂ showed lower power fade and better thermal safety than the LiNi_{0.8}Co_{0.15}Al_{0.05}O₂-based commercial cells under similar test conditions. Li-ion cells based on the material with excess lithium (Li_{1.1}Ni_{1/3}Co_{1/3}Mn_{1/3}O₂) exhibited excellent power performance that exceeded the FreedomCAR requirements.

© 2005 Elsevier B.V. All rights reserved.

Keywords: High-power Li-ion cell; Lithium manganese spinel; Li_{1+x}Ni_{1/3}Co_{1/3}Mn_{1/3}O₂; Lithium bisoxalato borate

1. Introduction

High-power lithium-ion batteries are promising alternatives to the nickel metal hydride (Ni-MH) batteries currently being used for energy storage in hybrid electric vehicles (HEVs). The use of lithium-ion batteries in the HEV systems is currently limited by their calendar life performance, thermal abuse characteristics, and cost. Under the Advanced Technology Development Program initiated by the U.S. Department of Energy (DOE) in 1998, Argonne National Laboratory (ANL) has developed high-power Li-ion cell chemistries utilizing lithium–nickel–cobalt oxide as the cathode and graphite as the anode. Although the cell chemistries with the lithium nickel cobalt oxide cathode initially meets the power requirements for the HEV applications [1], the Li-ion batteries using this cathode still possess concerns related to calendar life, safety, and cost. To address these barriers, ANL investigated high-power battery systems based

on two positive active materials that could offer low cost, long cycle, calendar life, and inherent safety. These two cathodes are based on Li_{1+x}Mn_{2-x}O₄ and Li_{1+x}Ni_{1/3}Co_{1/3}Mn_{1/3}O₂ with spinel and layered structures, respectively. In this article, we report ANL’s research efforts on the development and optimization of advanced Li-ion cells for high-power applications utilizing those two cathode materials.

2. The lithium manganese oxide spinel cathode material

Lithium manganese oxide spinels are very attractive cathode materials for high-power applications; they have excellent rate capability, due to their three-dimensional spinel framework, and could offer lower cost, longer calendar life, and better safety characteristics than the nickel system, e.g., LiNi_{0.8}Co_{0.2}O₂, due to superior stability of Mn⁴⁺ versus the Ni⁴⁺ in the charged electrode. However, it is well known that graphite/Li_{1-x}Mn₂O₄ lithium-ion cells suffer from significant capacity fade and impedance rise, particularly during

* Corresponding author. Tel.: +1 630 252 3838; fax: +1 630 972 4451.
E-mail address: amine@cmt.anl.gov (K. Amine).

Table 1

Concentration of Mn dissolved from stoichiometric (LiMn_2O_4) and substituted ($\text{Li}_{1.06}\text{Mn}_{1.94-x}\text{Al}_x\text{O}_4$) spinel powders stored in LiPF_6 - and LiBoB -based electrolytes at 55°C for 4 weeks

Materials	$\text{LiPF}_6/\text{EC}:\text{DEC}$ (ppm)	$\text{LiBoB}/\text{EC}:\text{DEC}$ (ppm)
LiMn_2O_4	64	0.05
$\text{Li}_{1.06}\text{Mn}_{1.94-x}\text{Al}_x\text{O}_4$	5	0.04

The Mn concentration was measured using the inductively coupled plasma (ICP) spectrometer

operation at elevated temperatures [2]. Thus, the spinel materials cannot be presently used for lithium-ion cells. The significant capacity fade of the lithium manganese oxide spinels at elevated temperatures is generally attributed to Mn dissolution from the spinel cathode induced by the presence of HF in the electrolyte [3]. Because the dissolution of Mn ions is closely related to the disproportionation of Mn^{3+} ($2\text{Mn}^{3+} \rightarrow \text{Mn}^{2+} + \text{Mn}^{4+}$), it is expected that substitution of Mn with other elements, such as Li and Al, will increase the average oxidation state of Mn ions, and thus, may suppress the Mn dissolution. Table 1 shows the effectiveness of the Li- and Al-substitution in reducing the Mn dissolution from the spinel materials. These studies indicate that the substituted spinel is much more resistant to Mn dissolution in the LiPF_6 -based electrolyte than the stoichiometric material. In fact, the substituted spinel exhibited significantly better capacity retention than the stoichiometric one at 55°C when they were cycled against Li-metal anode (data not shown here). When the substituted spinel was cycled versus graphite anode, however, significant capacity fade was still observed at elevated temperature. Fifty and 96% capacity retention versus the graphite and the Li-metal anode, respectively, were observed after 100 cycles at 55°C . To investigate the origin of the significant degradation of the graphite/substituted spinel cells in spite of the significant reduction of Mn ion dissolution, we measured the ac impedance of the cell during cycling at 55°C using a specially designed Li–Sn reference electrode [4]. The results of which are shown in Fig. 1. The ac impedance was measured after one formation cycle at room temperature (Fig. 1(a)) and after 25 cycles at 55°C (Fig. 1(b)). At the initial stages of cycling, the impedance of the negative electrode was much smaller than that of the positive electrode; however, after 25 cycles at 55°C , the impedance of the negative electrode increased significantly and overwhelmed that of the positive electrode. The graphite anode cycled in the Li-ion cell at 55°C was examined by energy dispersive spectroscopy (EDS). The EDS spectrum clearly showed the presence of Mn-metal on the graphite surface. It is thought that the small amount of dissolved Mn^{2+} (5 ppm) was reduced at the graphite surface, whose potential is ca. 0.08 V versus Li° , and played a catalytic role in forming a film at the graphite surface leading to the huge rise of interfacial impedance at the negative electrode. To prove this hypothesis, we performed a cycling experiment, using a $\text{Li}_4\text{Ti}_5\text{O}_{12}$ spinel anode, whose nominal voltage is ca.

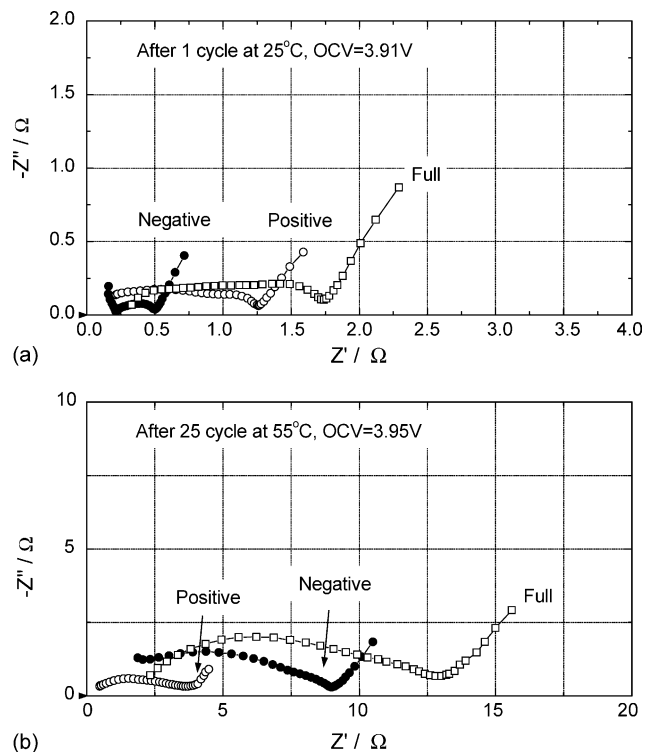


Fig. 1. Impedance of graphite/ $\text{Li}_{1.06}\text{Mn}_{1.94-x}\text{Al}_x\text{O}_4$ cell with Li–Sn alloy reference electrode (RE): (a) after 1 cycle at 25°C and (b) after 25 cycles at 55°C .

1.5 V versus Li° . Fig. 2 shows the cycling performance of the $\text{Li}_4\text{Ti}_5\text{O}_{12}/\text{Li}_{1.06}\text{Mn}_{1.94-x}\text{Al}_x\text{O}_4$ cell at 55°C . The result is that the $\text{Li}_4\text{Ti}_5\text{O}_{12}/\text{Li}_{1.06}\text{Mn}_{1.94-x}\text{Al}_x\text{O}_4$ cell exhibited excellent capacity retention (95% after 100 cycles) compared with the graphite/ $\text{Li}_{1.06}\text{Mn}_{1.94-x}\text{Al}_x\text{O}_4$ cell, which we attribute to the fact that the Mn^{2+} remains in the electrolyte solution and is not reduced on the $\text{Li}_4\text{Ti}_5\text{O}_{12}$ surface, due to its high reduc-

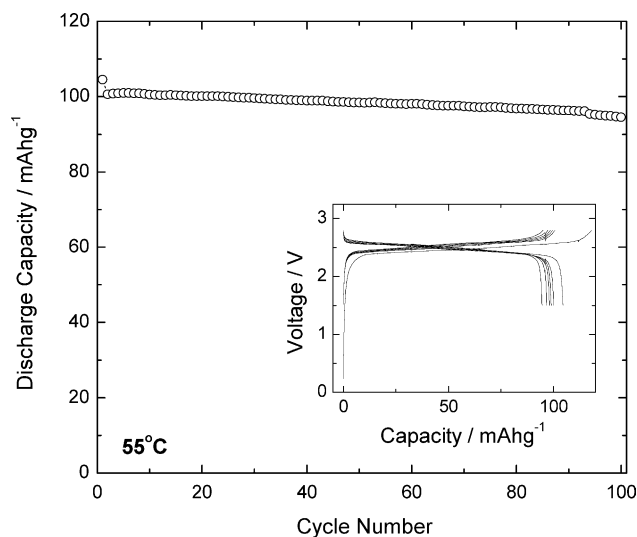


Fig. 2. Variation of discharge capacity against cycle number of $\text{Li}_4\text{Ti}_5\text{O}_{12}$ /substituted spinel cell cycled in the voltage range of 2.8–1.5 V. The charge/discharge curves are shown in the inset.

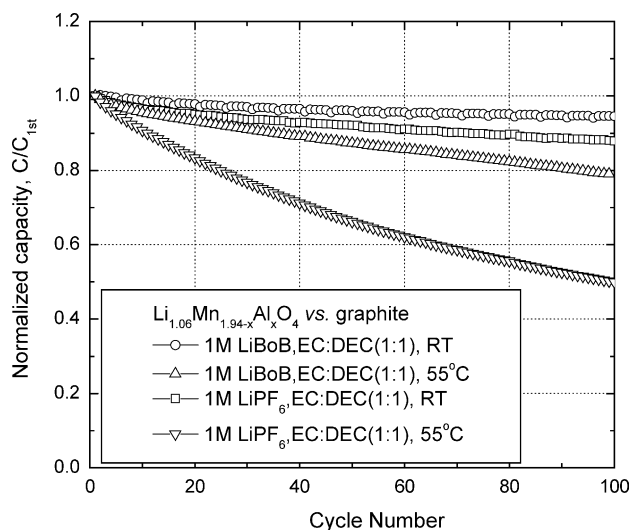


Fig. 3. Normalized discharge capacity against cycled number of graphite/substituted spinel cells using 1 M LiBoB/EC:DEC (1:1) electrolyte and 1 M LiPF₆/EC:DEC (1:1) electrolyte at RT and 55 °C. C_{1st} denotes the first discharge capacity.

tion potential. Therefore, for successful commercialization of the spinel cell system, it is necessary to either develop an alternative anode material on which the Mn^{2+} is not reduced, or an electrolyte system that does not produce an acidic environment, which causes the Mn^{2+} dissolution.

Recently, the LiBoB salt has been developed and studied as an alternative lithium salt to LiPF₆ for Li-ion cells [5,6]. The absence of fluorine in LiBoB has led us to consider it as an attractive lithium salt for use in graphite/spinel Li-ion cells because it will not produce a strong acidic environment. Hence, the Mn^{2+} dissolution should be suppressed. Table 1 shows the amounts of Mn dissolved from the stoichiometric and substituted spinel powders in the LiBoB/EC:DEC (1:1) electrolyte after a 4-week storage at 55 °C. As expected, only a negligible amount of manganese was detected for both spinel materials in the LiBoB-based electrolyte. Fig. 3 shows the capacity fade of the substituted spinel versus graphite at room temperature and 55 °C in the LiBoB- and LiPF₆-based electrolytes. The cycling performance of the graphite/substituted spinel Li-ion cell with LiBoB-based electrolyte was remarkably improved at 55 °C, which is consistent with the Mn leaching experiments. These results indicate that the spinel appears to be much more stable in the LiBoB-based electrolyte than it is in the LiPF₆ based electrolyte. However, we found that the graphite/substituted spinel cells with LiBoB/EC:DEC (1:1) electrolyte showed rather high impedance; the initial area specific impedance (ASI) of the cell using 1 M LiBoB/EC:DEC (1:1) electrolyte was about 40 Ωcm^2 , whereas that of similar cells using 1 M LiPF₆/EC:DEC (1:1) was only $\sim 28\text{ }\Omega\text{cm}^2$ [7]. The high ASI of the cell using 1 M LiBoB/EC:DEC (1:1) electrolyte is mainly due to the poor conductivity of this electrolyte as well as the preparative impurities present in the LiBoB salt used for this study. Through extensive efforts to purify the LiBoB

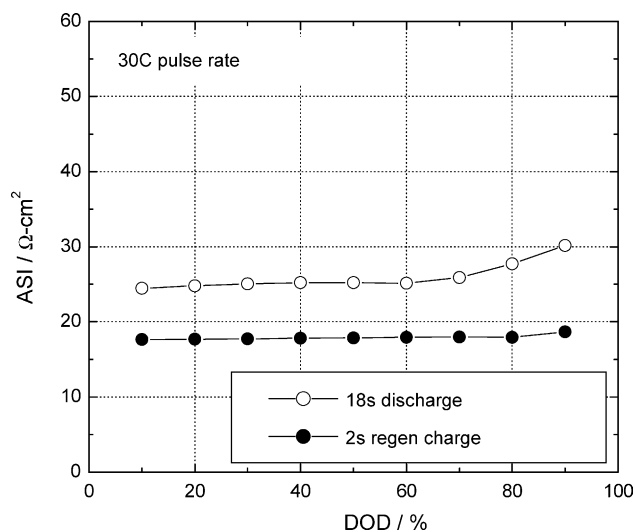


Fig. 4. The area specific impedance (ASI) of graphite/spinel cell with LiBoB/EC:PC:DMC (1:1:3) as a function of depth of discharge (DOD). The pulse current rate was 30C.

salt and to optimize the organic electrolyte solvents and their concentration, we have significantly improved the power characteristics of the cell system. In this work, we established that the 0.7 M LiBoB/EC:PC:DMC (1:1:3) electrolyte system had the highest lithium-ion conductivity and the lowest viscosity. Fig. 4 shows the ASI of the graphite/substituted spinel cell using the 0.7 M LiBoB/EC:PC:DMC (1:1:3) electrolyte; the ASI was measured using the FreedomCAR hybrid pulse power characteristic (HPPC) test at a 30C pulse current rate. The cell exhibited ASI values for both 18 s discharge and 2 s regenerative charge that far exceed the value required by the FreedomCAR HEV applications (35 and 25 Ωcm^2 , respectively). Although not shown here, the graphite/spinel cells using the LiBoB electrolyte also showed excellent aging characteristics and thermal safety. These results indicate that the lithium manganese oxide spinel, combined with LiBoB-based electrolyte, could provide high-power Li-ion batteries with low cost, good calendar life, and excellent thermal safety for HEV applications.

3. $\text{Li}_{1+x}\text{Ni}_{1/3}\text{Co}_{1/3}\text{Mn}_{1/3}\text{O}_2$ cathode material

The layered $\text{LiNi}_{1/3}\text{Co}_{1/3}\text{Mn}_{1/3}\text{O}_2$ (1/3–1/3–1/3) could be an alternative cathode to the commonly used $\text{Li}(\text{Ni}_{0.8}\text{Co}_{0.2})\text{O}_2$ and could offer longer calendar life for the HEV applications. The amount of active nickel in this material is small and the total oxidation of Ni to the tetravalent state takes place at 4.6 V. In addition, the Mn^{4+} cations in the structure play a stabilizing role preventing a structural collapse during cycling. By considering these two factors, we should expect a safer cell system with no phase segregation for the $\text{LiNi}_{1/3}\text{Co}_{1/3}\text{Mn}_{1/3}\text{O}_2$ system when operated within the voltage window of 3–4.2 V, which was one of the causes identified for power fade in the $\text{Li}(\text{Ni}_{0.8}\text{Co}_{0.2})\text{O}_2$ cathode

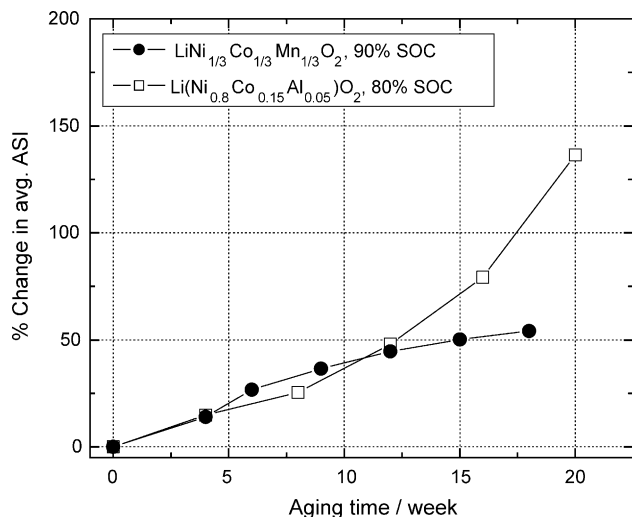


Fig. 5. Change of ASI during 55°C aging at 80–90% SOC of graphite/ $\text{LiNi}_{1/3}\text{Co}_{1/3}\text{Mn}_{1/3}\text{O}_2$ and graphite/ $\text{Li}(\text{Ni}_{0.8}\text{Co}_{0.15}\text{Al}_{0.05})\text{O}_2$ cells.

material when operated in this same voltage window [8–11]. Furthermore, it is anticipated that the $\text{LiNi}_{1/3}\text{Co}_{1/3}\text{Mn}_{1/3}\text{O}_2$ material will exhibit a significant decrease in thermal reactivity and a significant improvement in calendar life due to a very low Ni^{4+} content within the operating voltage window below 4.2 V. Fig. 5 shows the results of calendar life test at 55°C of 18,650 cells based on $\text{LiNi}_{1/3}\text{Co}_{1/3}\text{Mn}_{1/3}\text{O}_2$ and $\text{Li}(\text{Ni}_{0.8}\text{Co}_{0.15}\text{Al}_{0.05})\text{O}_2$. The 18,650 cells based on graphite/ $\text{LiNi}_{1/3}\text{Co}_{1/3}\text{Mn}_{1/3}\text{O}_2$ were potentiostated at 90% state of charge (SOC) and aged at 55°C over 15 weeks. On the other hand, the 18,650 cells based on graphite/ $\text{Li}(\text{Ni}_{0.8}\text{Co}_{0.15}\text{Al}_{0.05})\text{O}_2$ were potentiostated only at 80% SOC and aged at 55°C for 20 weeks. The results show that the ASI of the cell based on $\text{LiNi}_{1/3}\text{Co}_{1/3}\text{Mn}_{1/3}\text{O}_2$ increased by about 50% and then stabilized. However, the ASI of the cell based on $\text{Li}(\text{Ni}_{0.8}\text{Co}_{0.15}\text{Al}_{0.05})\text{O}_2$ continued to grow with aging time and increased by 120% after 20 weeks of aging. Fig. 6 shows the differential scanning calorimetry (DSC) curves of $\text{Li}(\text{Ni}_{0.8}\text{Co}_{0.15}\text{Al}_{0.05})\text{O}_2$ and

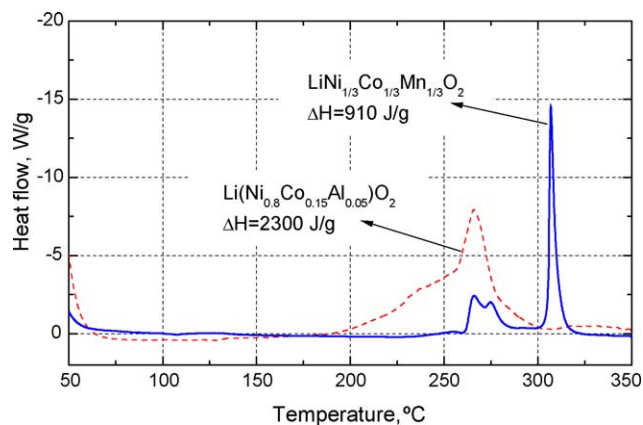


Fig. 6. Differential scanning calorimetry (DSC) profile ($10^\circ\text{C min}^{-1}$) of $\text{LiNi}_{1/3}\text{Co}_{1/3}\text{Mn}_{1/3}\text{O}_2$ and $\text{Li}(\text{Ni}_{0.8}\text{Co}_{0.15}\text{Al}_{0.05})\text{O}_2$ charged to 4.3 V.

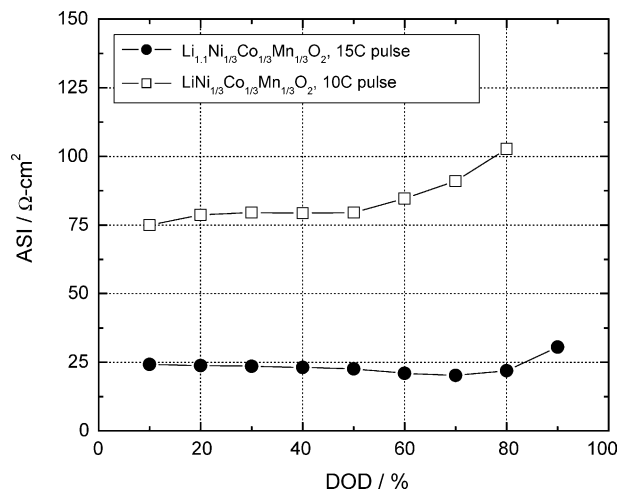


Fig. 7. The area specific impedance (ASI) of graphite/ $\text{LiNi}_{1/3}\text{Co}_{1/3}\text{Mn}_{1/3}\text{O}_2$ and graphite/ $\text{Li}_{1.1}\text{Ni}_{1/3}\text{Co}_{1/3}\text{Mn}_{1/3}\text{O}_2$ cells with $\text{LiPF}_6/\text{EC}:\text{PC}:\text{DMC}$ (1:1:3). The pulse current rate was 10C and 15C, respectively.

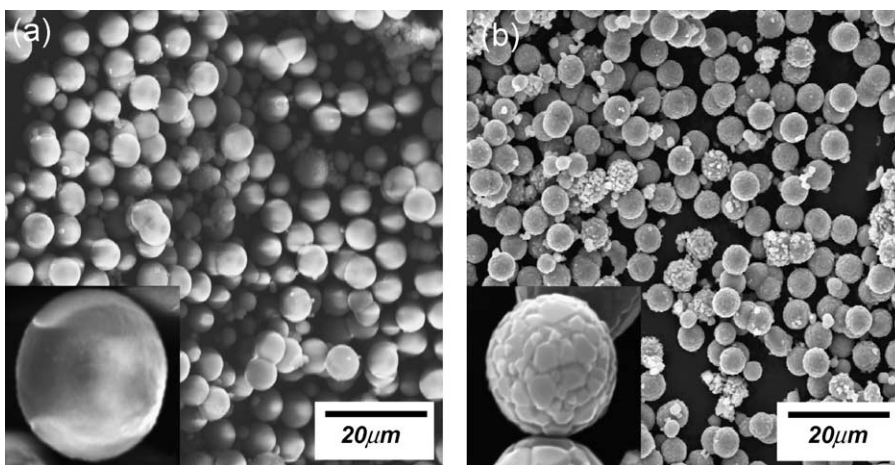


Fig. 8. SEM images of (a) $(\text{Ni}_{1/3}\text{Co}_{1/3}\text{Mn}_{1/3})\text{CO}_3$ precursor and (b) $\text{Li}_{1.1}\text{Ni}_{1/3}\text{Co}_{1/3}\text{Mn}_{1/3}\text{O}_2$ calcined at 1000°C using the carbonate precursor.

$\text{LiNi}_{1/3}\text{Co}_{1/3}\text{Mn}_{1/3}\text{O}_2$ cathode materials charged to 4.3 V with LiPF_6 -based electrolyte. Figs. 5 and 6 clearly show that the $\text{LiNi}_{1/3}\text{Co}_{1/3}\text{Mn}_{1/3}\text{O}_2$ cell system exhibits much better calendar life and thermal safety characteristics than the $\text{Li}(\text{Ni}_{0.8}\text{Co}_{0.15}\text{Al}_{0.05})\text{O}_2$ system. However, the HPPC test revealed that the graphite/ $\text{LiNi}_{1/3}\text{Co}_{1/3}\text{Mn}_{1/3}\text{O}_2$ cell did not meet the power requirements of the FreedomCAR partnership. To improve the power performance of the material, we investigated the effect of excess lithium on the performance to the $\text{Li}_{1+x}\text{Ni}_{1/3}\text{Co}_{1/3}\text{Mn}_{1/3}\text{O}_2$ material. Fig. 7 compares the ASI values of the stoichiometric ($x=0$) and lithium excess ($x=0.1$) materials measured by the HPPC test. The material with excess lithium exhibits excellent pulse power rate capabilities that exceed the FreedomCAR requirements. Further studies are currently under way to develop a high-power Li-ion cell chemistry using the $\text{Li}_{1+x}\text{Ni}_{1/3}\text{Co}_{1/3}\text{Mn}_{1/3}\text{O}_2$ cathode material. At the same time, we are developing a new synthesis process, using carbonate precursors, to obtain a highly dense and spherical $\text{Li}_{1+x}\text{Ni}_{1/3}\text{Co}_{1/3}\text{Mn}_{1/3}\text{O}_2$ material, an example of which is shown in Fig. 8.

4. Summary and conclusions

In spite of the very limited Mn^{2+} dissolution of substituted lithium manganese oxide spinel ($\text{Li}_{1.06}\text{Mn}_{1.94-x}\text{Al}_x\text{O}_4$) in the electrolyte, the graphite/spinel Li-ion cells using LiPF_6 -based electrolyte still showed severe capacity fade at 55 °C. Our ac impedance measurements, with a Li–Sn reference electrode cell, indicated that the bulk of the impedance was occurring at the graphite electrode. The EDS study of the graphite anode cycled in the Li-ion cell indicated that Mn^{2+} ions were reduced to Mn-metal on the graphite anode surface, which we believe caused the increase in the charge-transfer impedance at the anode/electrolyte interface. We propose this reduction as the main degradation mechanism of the graphite/spinel Li-ion cells. The LiBoB salt was investigated as an alternative to LiPF_6 for the graphite/spinel Li-ion cells. The Li-ion cells employing the LiBoB-based electrolyte exhibited superior performance relative to the cells with LiPF_6 -based electrolyte in their cycle/calendar life and thermal safety.

$\text{Li}_{1+x}\text{Ni}_{1/3}\text{Co}_{1/3}\text{Mn}_{1/3}\text{O}_2$ was also investigated as a potential cathode material for high-power Li-ion battery systems that could offer lower cost, improved safety, and better performance than the $\text{LiNi}_{0.8}\text{Co}_{0.15}\text{Al}_{0.05}\text{O}_2$ cell system. Calendar life and thermal safety test of graphite/ $\text{Li}_{1+x}\text{Ni}_{1/3}\text{Co}_{1/3}\text{Mn}_{1/3}\text{O}_2$ cells showed lower power fade and better thermal safety than the graphite/ $\text{LiNi}_{0.8}\text{Co}_{0.15}\text{Al}_{0.05}\text{O}_2$ cell system. Excellent power performance was also observed from the material with excess lithium ($\text{Li}_{1.1}\text{Ni}_{1/3}\text{Co}_{1/3}\text{Mn}_{1/3}\text{O}_2$). Such Li-ion cells exhibited power performance that exceeded the FreedomCAR requirements.

Acknowledgement

The authors acknowledge the financial support of the U.S. Department of Energy, FreedomCAR & Vehicle Technologies Program under Contract No. W-31-109-Eng-38.

References

- [1] C.H. Chen, J. Liu, M.E. Stoll, G. Henriksen, D.R. Vissers, K. Amine, *J. Power Sources* 128 (2004) 278.
- [2] K. Amine, J. Liu, S.-H. Kang, I. Belharouak, Y. Hyung, D. Vissers, G. Henriksen, *J. Power Sources* 129 (2004) 14.
- [3] D.H. Jang, Y.J. Shin, S.M. Oh, *J. Electrochem. Soc.* 143 (1996) 2204.
- [4] D.P. Abraham, J. Liu, C.H. Chen, Y.E. Hyung, M. Stoll, N. Elsen, S. MacLaren, R. Twesten, R. Haasch, E. Sammann, I. Petrov, K. Amine, G. Henriksen, *J. Power Sources* 119 (2003) 511.
- [5] W. Xu, C.A. Angell, *Electrochem. Solid State Lett.* 4 (2001) 1.
- [6] K. Xu, S. Zhang, T.R. Jow, W. Xu, C.A. Angell, *Electrochem. Solid State Lett.* 5 (2002) A26.
- [7] K. Amine, J. Liu, Proceedings of the First International Conference on Polymer Batteries and Fuel Cells, Jeju, Korea, June 1–6, 2003, p. INV 14 (extended abstract).
- [8] K. Amine, C.H. Chen, J. Liu, M.J. Hammond, A.N. Jansen, I. Bloom, D.R. Vissers, G.L. Henriksen, *J. Power Sources* 97–98 (2001) 684.
- [9] D.P. Abraham, R.D. Twesten, M. Balasubramanian, J. Kropf, D. Foscher, J. McBreen, I. Petrov, K. Amine, *J. Electrochem. Soc.*, in press.
- [10] D.P. Abraham, R.D. Twesten, M. Balasubramanian, I. Petrov, J. McBreen, K. Amine, *Electrochem. Commun.* 4 (2002) 620.
- [11] A.M. Andersson, D.P. Abraham, R. Haasch, S. MacLaren, J. Liu, K. Amine, *J. Electrochem. Soc.* 149 (2002) A1358.